EFESTO - advancing European hypersonic inflatable heatshield technology for Earth recovery and Mars highmass delivery missions

MedCrave
Step into the World of Research

Aeronautics and Aerospace Open Access Journal

Research Article

Open Access

CrossMark

EFESTO - advancing European hypersonic inflatable heatshield technology for Earth recovery and Mars high-mass delivery missions

Abstract

The European Union H2020 EFESTO project is coordinated by DEIMOS Space with the end goals of improving the European TRL of Inflatable Heat Shields for re-entry vehicles (from 3 to 4/5) and paving the way towards further improvements (TRL 6 with a future In-Orbit Demonstrator). This paper presents the project objectives and provides with a general overview of the activities ongoing and planned for the next two years, promoting its position in the frame of a European re-entry technology roadmap. EFESTO aims at (1) the definition of critical space mission scenarios (Earth and Mars applications) enabled by the use of advanced inflatable Thermal Protection Systems (TPS), (2) characterization of the operative environment and (3) validation by tests of both the flexible materials needed for the thermal protection (flexible thermal blanket will be tested in arcjet facility in both Earth and Martian environments) and the inflatable structure at 1:2 scale (exploring the morphing dynamics and materials response from packed to fully inflated configuration). These results will be injected into the consolidated design of a future In-Orbit Demonstrator (IOD) mission.

Keywords: heat shields, finite element model, earth application, material emissivity, radiative heat flux

Volume 6 Issue 2 - 2022

Giuseppe Guidotti,[1] Irene Pontijas Fuentes,[1] Federico Trovarelli,[1] Ingrid Dietlein,[2] Thorn Schleutker,[2] Roberto Gardi,[3] Jean-Luc Verant,[4] Ysolde Prevereaud,[4] Yann Dauvois,[4] Giuseppe Governale[5]

[1]DEIMOS Space S.L.U, Spain
[2]Deutsches Zentrum für Luft- und Raumfahrt e.V. (DLR), Germany
[3]Centro Italiano Ricerche Aerospaziali (CIRA), Italy
[4]Office National d'Etudes et de Recherches Aerospatiales (ONERA), France
[5]Department of Mechanical and Aerospace Engineering, Politecnico di Torino, Italy

Correspondence: Giuseppe Governale, Department of Mechanical and Aerospace Engineering, Politecnico di Torino, Italy, Tel +39 3490024133, Email giuseppe.governale@polito.it

Received: June 9, 2022 | **Published:** July 4, 2022

Abbreviations

AOA, angle of attack; AVUM, attitude and vernier upper module; BC, ballistic coefficient defined as mass/(drag coefficient * reference surface), kg/m^2; CAD, computed aided design; CGG, cold gas generator; COG, centre of gravity; D&L, descent and landing; ESA, European space agency; F-TPS, flexible thermal protection system; FEM, finite element model; FS, front shield; GNC, guidance navigation and control; H2020, horizon 2020 is the financial instrument implementing the innovation union a Europe 2020 flagship initiative aimed at securing Europe's global competitiveness; HIAD, hypersonic inflatable aerodynamic decelerator; IAD, inflatable aerodynamic decelerator; IOD, in-orbit demonstrator; IXV, intermediate experimental vehicle (re-entry demonstrator); MAR, mid air retrieval; MOLA, mars orbiter laser altimeter; NASA, National aeronautics and space administration; SRP, supersonic retro propulsion; SSO, sun synchronous orbit; TPS, thermal protection system; TRL, technology readiness level; ULA, united launch alliance; VEGA, European vector of advanced generation

Introduction

FULLY in line with the European Union H2020 call SPACE-11-TEC-2018, EFESTO will provide advances in the three areas of thermal control, materials and structures through the design and testing of innovative inflatable TPS solutions for re-entry vehicles. It will enable new space mission concepts, which require bringing a payload from space to ground of a planetary body with an atmosphere beyond the current limits imposed by launcher fairing size or rigid heat shields geometrical and structural aspects. Morphing solutions will allow for example landing bigger or heavier payload on Mars or will enable the reusability of launchers' upper stages enhancing European reusability and cost reductions in the access to space industry. Non space applications in the areas of materials and structures will also be considered.

Leveraging on the consortium background and on past, current and planned test results in the field, competitiveness in the space sector will be fostered and key contributions to the long-term European re-entry technology roadmap will be provided. EFESTO is built on four key technical elements (red bullets in Figure 1 which shows the high-level EFESTO study logic) to advance from the current European state of art to the preparation of an IOD mission, overall increasing the TRL of this technology in Europe. In the first year of activities, the focus has been on the missions and system design, including preliminary structure and TPS design and supported by aerothermodynamic simulations. The status of the current design solutions for two key applications (Mars Robotic Exploration and Reusable Small Launchers Upper Stages) is presented.

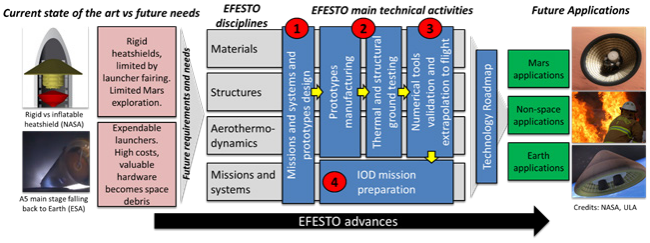

Figure 1 EFESTO study logic and key elements (red circles).

For the Mars Application, the robotic exploration mission class resulted in a 10 m diameter IAD class, with about 6600 kg of entry mass, and a BC of about 50 kg/m^2. The current mission (see Figure 2) foresees a direct Mars entry and combines the use of hypersonic IAD (HIAD) in a ballistic entry (e.g., with an angle of attack of zero degree maintained along the entry trajectory) with Supersonic Retro-Propulsion (SRP, activated about Mach 2.3) to deliver about 2500 kg of payload at a landing altitude of MOLA +2 km.

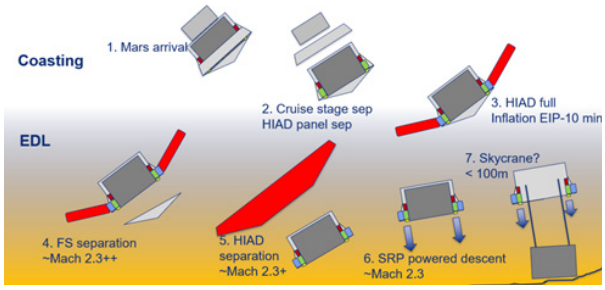

Figure 2 Mars application: concept of operations. EFESTO focus is on the HIAD design and flight phases.

For the Earth Application, the VEGA upper stage (AVUM) has been selected as baseline study case. The current mission (see Figure 3) foresees a deorbiting from SSO orbit, a controlled lifting entry phase (BC of about 30 kg/m2 and a 15° of AoA maintained along the entry phase) and combines the use of hypersonic IAD (HIAD, 4.5m diameter class) with parachutes and parafoil for Mid-Air-Capturing (MAR) with a helicopter. Refurbishment of the recovered stage is planned as necessary step before a re-flight of the launcher stage.

Figure 3 Earth application: concept of operations. EFESTO focus is on the HIAD design and flight phases.

Following the ongoing design phases, the next project steps will include laboratory tests as preparatory activities for a future In-Orbit Demonstrator mission. Test in DLR arc-heated facility LBK will be reconstructed by numerical simulations to assess the heat and mass transfer interaction between the material and the flow field. Tests in CIRA facility of the inflatable structure will be reconstructed by numerical simulation to validate structural models. The current status is presented.

Placing the future IOD mission in the context of a broader and longer-term technology context is also one of the project goals, open and willing to find synergies with ongoing and future efforts in the European context.[1]

I. State of the art

On the European scenario, the last mission to fly an inflatable heatshield technology demonstrator was the Inflatable Reentry and Descent Technology (IRDT); an ESA/Russia mission that performed two test flights, in 2000 and 2005, however both resulted in hard landing and loss of the capsule with only partial telemetry recovered.[2] Since 2005, European studies of the likes of STEP2 (2014), IRENA (2015), HYPMOCES (2016) and IAD/DAD (2017) have been focused on lower TRLs, considering the design and specimen testing of inflatable components and flexible TPSs never foreseeing neither a scaled system testing nor demonstration flights.

In the worldwide context, over the last two decades, NASA has continuously and steadily increased the TRL of inflatable heatshield and flexible TPS technology though the IRVE[3] and HIAD[4] studies. IRVE-3 in 2012 performed a successful demo mission after flying a suborbital arc, re-entering at a velocity of Mach 10 and reaching 1000ºC of temperature on the inflated heatshield. NASA is currently building on the experience gained on the stacked toroid configuration and flexible TPS materials, pushing the technology forwards with programs such as LOFTID[1] and SMART.[5] The first is currently developing and in-orbit demonstrator of 6 m diameter and is designed to re-enter from orbital velocities, both for Earth and Mars applications, while the latter is the result of NASA and ULA joint efforts to develop the technology for re-usability of launcher stages.

Other than the US, also China is developing inflatable decelerators with a Flexible Inflatable Cargo Re-entry Vehicle. Recently tested in 2020. The vehicle with a deployed HIAD of 3 m in diameter suffered an anomaly during entry, however this demonstrates the level of progress also from the Chinese in the development of the technology.

Overall, the literature shows that both the US and China are developing and testing with demo-mission the capabilities of inflatable structures and flexible TPS for hypersonic flight deceleration and heat shielding of the payload. NASA is focusing on possible Mars entry applications with LOFTID and Earth launcher stages recovery with SMART. China is also developing the technology and is currently performing in-orbit demonstration mission. At European level, the TRL is lower and since the partial failures of the IRDT mission, only preliminary studies have been performed. The EFESTO project shall lift the European TRL from 3 to 4 or 5 by performing ground tests of material specimen and full-scale IAD concept tests in preparation to a European in-orbit demonstration (IOD) that shall allow increasing the TRL further to 6. In preparation to the latter, EFESTO will define an IOD mission, the results being expected by the end of the present project.

II. System design

Several system design loops were run for both study cases beginning with first decisive preliminary trade-offs during a concurring engineering activity using the DLR Concurrent Engineering Facility in Bremen and now having reached the detailed design stage. A suitable HIAD design and integration had to be found showcasing the applicability of this technology for these two distinct application cases. Additionally, both study cases serve for deriving relevant requirements towards the system design and for the integration of the HIAD. This section presents the current status of the system design for both study cases and highlights relevant points and requirements as identified during the design loops.

Earth application

The compact design of AVUM renders it particularly suitable for the selected application since it offers two major benefits with respect to the design for reentry:

a) Comparatively forward position of the stage center of gravity in comparison to more elongated rocket stages, which is beneficial for flight stability during reentry.

b) Reduced exposure to wake flow downstream of the inflatable heat shield.During the design process, several challenges had to be overcome:

c) Integration of the folded HIAD in ascent configuration with the commercial VEGA payload on top providing sufficient volume to the packed HIAD.

Citation: Guidotti G, Fuentes IP, Trovarelli F, et al. EFESTO - advancing European hypersonic inflatable heatshield technology for Earth recovery and Mars high-mass delivery missions. *Aeron Aero Open Access J.* 2022;6(2):59–73. DOI: 10.15406/aaoaj.2022.06.00142

d) Conflicting requirements with respect to the lateral position of the center of gravity during ascent and descent. During ascent, the lateral deviation of the CoG from the symmetric axis is limited. According to the VEGA User Manual the maximum deviation for a payload is limited to below 15 mm, see.[6] During descent, however, the required lateral deviation shall be ~ 0.2 m to trim around 15º AoA and produce enough aerodynamic lift for controlling the vehicle during re-entry. This is needed to target precise conditions at parachuted deployment.

e) Integration of the Descent & Landing system to the stage.The retained design features for the Earth Application, alongside the HIAD, include the use of an internal cone transmitting the reentry forces on the inflated HIAD to the stage structure, an IAD external cone (IEC) carrying the payload similar to the VEGA's VAMPIRE or VESPA to be jettisoned prior to inflation, a cold gas generator system (CGG) to provide the inflation gas and a descent & landing (D&L) system consisting of a pilot chute, supersonic drogue chute and a parafoil for final descent phase before being captured by a helicopter. Figure 4 presents an overview of the system in reentry configuration (nose radius: 1,3m, cone angle 120°).

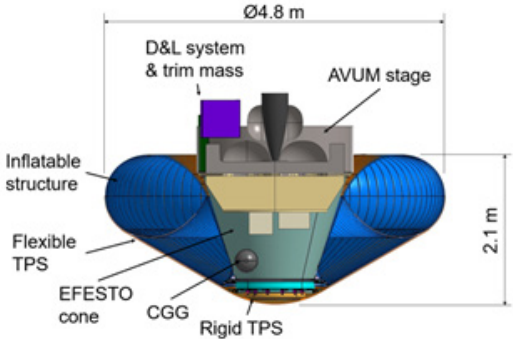

Figure 4 EARTH application: AVUM with inflated HIAD in re-entry configuration.

Several options exist in order to overcome the contradiction with respect to the requirements for the lateral CoG displacement, ranging from design measures such as tilting the AVUM with respect to the inflated HIAD to the use of a movable mass or aerodynamic trim tabs. As baseline option for the Earth application the use of a static trim mass was preferred due to its simplicity. Shifting laterally the position of the D&L system and the CGG will limit the mass required for reentry trim. A second trim mass is to be foreseen in order to obtain a CoG close to the symmetric axis during ascent. This additional trim mass has to be jettisoned prior to reentry and, for this reason, is ideally integrated into the IAD external cone. Figure 5 provides an overview of the mass distribution for the reentry mass.

As it can be seen, the HIAD system is very light itself and shows the benefit of this technology. At the same time the structural components for integrating the HIAD to AVUM is playing a significant role in the overall budget. However, as a result of the preliminary nature of this feasibility study there are still considerable vectors for optimizing the structural parts. A further mass driver is the reentry trim mass that amounts to 15% of the entire reentry mass. Other solutions should therefore be investigated in the future such as inclining the cone formed by the inflated HIAD which could avoid adding a trim mass to the system.

Mars application

The detailed design phase of the Mars application system is still going on but the principal design choices have been settled in what concerns the overall architecture. Figure 6 presents an overview of the architecture resulting from the preliminary design phase (nose radius: 1,75 m, cone angle 140°). The scientific payload (envelope: diameter 2.8 m, height 2.5 m, mass 2.5T) is hosted by a carrier frame (blue) equipped with the supersonic retro-propulsion (SRP) system including the fuel and helium tanks, avionics and the crane equipment used to lower the scientific payload to the Mars surface similarly to the Skycrane maneuver. It also provides storage volume to the packed HIAD and transmits forces from the HIAD during reentry and from the propulsion system to the scientific payload. The heatshield protecting the payload and the descent module subsystems from the reentry environment will be separated during the descent, see Figure 2.

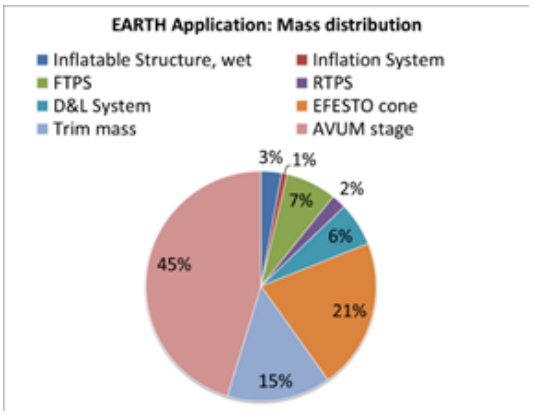

Figure 5 Mass distributions for the re-entry configuration of the AVUM study case.

For the propulsion system the use of Aerojet Rocketdyne's MR-80B3100 thruster is a suitable off-the-shelf option considered for this study case. It can be operated with hydrazine and may be throttled between 31 N and 3601 N.[7] This engine may also be operated with the better performing bipropellant MMH/N2O4 fuel combination allowing the saving of several hundred kilograms of fuel mass. However, as the engine in combination with this bipropellant fuel is not flight proven to this date, it was decided to build the system around the monopropellant fuel option as baseline. The thrusters are fired at approximately Mach 2.3 (also not proven to date yet on Mars in SRP conditions) to decelerate the descent module after an aerodynamic deceleration phase until the descent speed is zero after the front heat shield and the inflatable structure are separated. The payload then is lowered to the surface from the stationary descent module. The mass of the descent module including the scientific payload is distributed as shown by Figure 7.

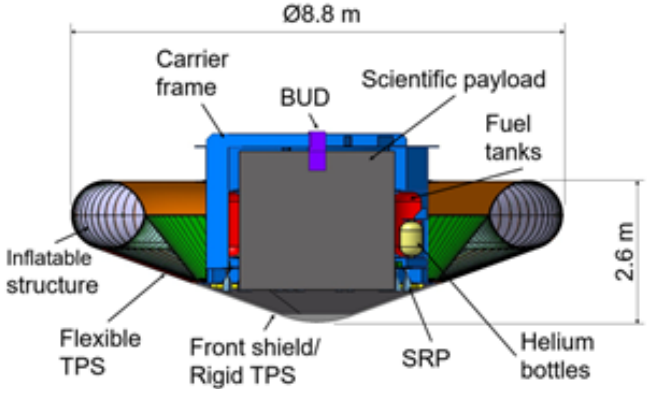

Figure 6 MARS application: Descent module after release (HIAD in packed configuration).

Citation: Guidotti G, Fuentes IP, Trovarelli F, et al. EFESTO - advancing European hypersonic inflatable heatshield technology for Earth recovery and Mars high-mass delivery missions. *Aeron Aero Open Access J.* 2022;6(2):59–73. DOI: 10.15406/aaoaj.2022.06.00142

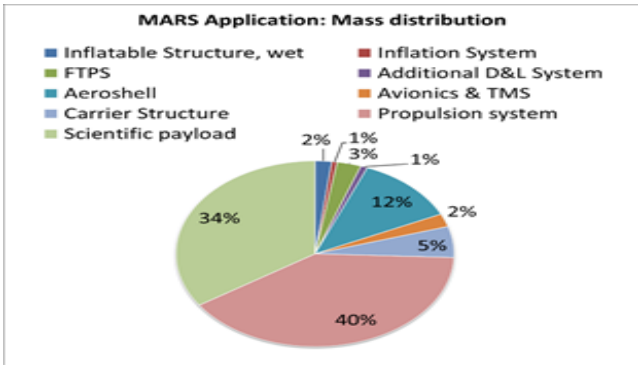

Figure 7 Mass distribution for the re-entry configuration of the MARS study case.

Again, the HIAD itself contributes comparatively little to the entire system mass. It is the structural parts, in particular the aeroshell, but above all the propulsion system with nearly 40% of mass contribution that drive the system mass. It shall however be recalled that the propulsion system mass is based on the low performing monopropellant. A significant mass improvement can be obtained when switching to bipropellant fuel. A reduction of system mass of at least 10% seems then feasible. This would lead to further mass savings as the ballistic coefficient will decrease further requiring reduced heat shield diameter.

III. Aerodynamics and aerothermodynamics

Computational strategy

As explained in section III, several systems designs have been investigated from the beginning of the EFESTO project. To efficiently investigate all the options, the strategy focused on two kinds of code: ARES and CEDRE.

The ONERA engineering code ARES (Atmospheric Re-Entry Software) couples 4 independent codes: MUSIC (flight mechanics solver), FAST,[8,9] (aerodynamics and aerothermodynamics solver), AtMoS (atmospheric conditions solver) and MoDeTheC (heat and mass transfers as well as thermal degradation within the material). In the first part of this project, only FAST is considered to quickly calculate aerodynamic force and moment coefficients as well as wall heat flux at specific flight points or along complete Earth and Mars atmospheric entry trajectories. By using reduced order models FAST allows to quickly investigate several HIAD shapes to design the optimal trajectory with the flexible TPS. However, more or less important uncertainties are associated with the results of order reduced models. These uncertainties must therefore be quantified by comparing the results obtained by these engineering models with experimental and numerical data. Moreover, engineering codes do not allow studying the impact of complex physical phenomena such as separation zones or vortices on wall variables.

So, the ONERA CFD (Computational Fluid Dynamics) code CEDRE[10] is used to estimate and apply uncertainties inherent to the method used in ARES and also to investigate complex physical phenomena as radiative heat transfer from the high energy shock layer for Martian entry or possible wake flow impingement.

In the first part of this project, CFD computations have been performed in continuum hypersonic and supersonic regime only, since the most important aerothermodynamic constraints are encountered in hypersonic continuum regime. Moreover, at the end of re-entry, a supersonic parachute is deployed for the Earth mission and Supersonic Retro-Propulsion is ignited for Mars mission. The continuum regime is assumed for Knudsen number Kn – defined as the ratio between the mean free path λ (in m) and a reference length L_{ref} (in m) – inferior to 10^{-3}. For sphere-cones with high half cone angles ($\delta = 70°$ for the Mars mission and $\delta = 60°$ for the Earth mission) and flying at low angle of attack ($\alpha = 0°$ for Mars and $\delta = 15°$ for Earth), the diameter of the cone may be an appropriate reference length. So, the continuum regime is sensitive to both HIAD at an altitude of ~80 km on Earth and ~ 67 km on Mars.

Computational methods

For FAST[8,9] calculations, in continuum hypersonic regime, the modified Newtonian model has been used to compute the wall pressure distribution whose integration over the entire surface provides the aerodynamic force and moment coefficients. The stagnation convective-diffusive heat flux is obtained thanks to Sutton-Graves,[11] Fay-Riddell[12] or Vérant-Sagnier[13] equations. Then, the heat flux distribution along the wall is computed using Vérant-Lefrançois model[14] an ONERA in-house model. For Earth re-entries, wall convective-diffusive heat flux assuming catalytic, non-catalytic or partially catalytic wall can be calculated, while for Mars entry, only catalytic wall can be considered so far. All these models assume a laminar flow. In free-molecular flow regime, Bird's equations[15] are used to calculate pressure, skin friction and wall heat flux distributions. In rarefied regime, bridging functions allow to determine the aerodynamic coefficient and wall heat flux.

CEDRE[10] is a multi-physics platform coupling dedicated solvers, as CHARME to simulate reactive flow and ASTRE to compute the shock layer radiation. In the CHARME solver, Navier-Stokes equations have been resolved with a second-order finite-volume discretization in space on generalized unstructured meshes, with the flux vector splitting AUSM+ scheme associated to a Van Leer limiter. The time integration has been set to a one-step fully implicit approach. Computations have been then performed within both laminar or turbulent boundary layer assumptions. In this last case, computations have been done assuming a fully turbulent flow with the k-□□SST Menter model (two-equation model). A chemical non-equilibrium model based on Park's kinetics (5 species [O_2, N_2, N, O , NO] and 17 reactions for Earth, 5 species [CO_2, CO, O_2, O, C] and 18 reactions for Mars) is used. But, the state of the gas is not imposed and local gas equilibrium, freezing or nonequilibrium solutions are then a consequence of the local flow conditions. Similarly, using a 5 species gas model with corresponding dissociation, recombination and exchange reactions does not mean that all species are present in the flow nor that all reactions occur. However, vibrational/Electronic modes are assumed at equilibrium with Translational/Rotational mode.

Radiative computations follow a "two-ways" coupling between CHARME and ASTRE solvers, meaning that radiation flux absorbed by the surface is taken into account to update thermal balance at the wall. ASTRE is a radiative transfer solver based on a Monte Carlo method consisting in following a finite large number of energy bundles (an energy bundle is a discrete amount of energy, which can be thought as a group of photons bound together) through their transport histories, from their points of emission to their points of absorption (here IAD walls). In the present application, 5.6x108 numerical photons or energy bundles have been tracked. Radiation gaseous species model is based on CO_2 and CO molecules only since Mars atmospheric model is assumed to be composed of 100% CO2 upstream of the shock layer volume (4% N_2 contribution is

not significant at this stage of the project and unaccounted for). The radiative model used is a Statistical Narrow Band Model (SNB) which includes 450 spectral bands between 187.5 and 30262.5 cm^{-1}.

For all computations, the wall temperature has been calculated assuming the radiative equilibrium at the wall with a total emissivity of 0.8 relevant to Hi-Nicalon outer fabric and its probable oxidized coating.

Aerodynamics

The objective of the aerodynamic analysis is mainly to build an aerodynamic database used by other disciplines, in particular by the mission analysis to define the reference trajectory and the expected range of sizing flight conditions (see V). Moreover, the knowledge of the pressure distribution is necessary to ensure that the correct inflation of the structure is maintained along the complete atmospheric entry (see VII).

The design of the heat shield and in particular the inflatable structure has a significant influence on the aerodynamic forces and moments coefficients. The heat shield being a sphere-cone for the Earth and Mars missions, different geometrical parameters (Figure 8), often noticed in literature[16,17] influence the aerodynamics of the object, such as the half-cone angle δ or the bluntness which is the ratio between the nose radius R_n and the base radius R_b. Moreover, flight parameters, as the angle of attack α, and upstream flow characteristics, as Mach and Reynolds numbers, have obviously a major impact on the aerodynamics of the object.

Aerodynamics coefficients obtained with CEDRE and ARES have been compared among each other but also to experimental results from literature for Earth[17] and Mars[18] missions. Results obtained with CEDRE are in good accordance with the experimental results from literature. Moreover, a discrepancy less than 5% is observed between CEDRE and ARES results for the drag coefficient in hypersonic regime. This discrepancy increases significantly while getting closer to the supersonic regime. Thus, in this flow regime, complementary CFD simulations have been performed to complete the aerodynamic database.

Blunt body aerodynamics is generally dominated by the forebody shape in hypersonic and high supersonic regimes. Indeed, the relative error between aerodynamic coefficients calculated considering the forebody only or the full geometry varies from 0.04% to 0.4%; so a maximal absolute difference of 0.0015 on the drag coefficient is noticed. The stagnation point pressure is well predicted by ARES with a maximum relative discrepancy of around 1.4%. The pressure distribution on the conical part is underestimated by engineering formulations of around 8.5% at Mach 10 and 3.5% at Mach 25.

An analysis of the aerodynamic database was performed to evaluate the flying qualities associated to different shapes explored in the conceptual and preliminary design phases. The overall key performances monitored as a function of the CoG location were the trim angle (total AoA), the aerodynamic efficiency (L/D), and the trim stability (static margin). All these performances affect the system design on side (CoG location, and in particular the lateral CoG offset) and the mission performance (and business case, in particular the operations) on the other side. Overall a minimum L/D of about 0.15-0.2 is desirable for the controlled entry phase of the AVUM application, while ballistic entry around AoA = 0º is enough for Mars.

Aerothermodynamics

The objective of the aerothermodynamic (ATD) analysis is to forecast the heat load received by the wall all along the defined trajectory. The both wall heat flux distribution and the stagnation point heat flux are subsequently used for F-TPS membrane (see VI) and IAD Inflatable Structure (see VII) design sizing values. The wall heat flux is highly dependent on the design of the object, in particular (see Figure 8), the nose radius R_n, the half cone angle δ but also the base radius R_b (radiative heat transfer from the shock layer), but also obviously on the upstream flow conditions, as density ρ_∞, velocity V_∞.

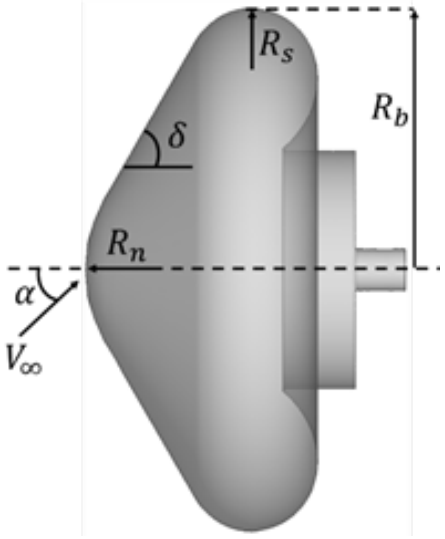

Figure 8 Geometrical parameters.

Simulations have been led to investigate the influence of the wall catalysis, the material emissivity, the turbulence on the blunt cone, the wake environment, and the shock layer radiation on the wall heat load for Earth and Mars missions.

Wall catalysis

Surface catalysis is of primary importance in the design of the TPS material since the wall catalysis can be a significant source of diffusive-convective heating release during re-entry. Its influence is important for highly dissociated flow, e.g. when the mass fractions of the atomic species in the shock layer are significant. On the major part on the entry trajectories, the convective-diffusive heat flux assuming a full catalytic wall is more than twice higher than the non-catalytic wall heat flux, not only at the stagnation point (Figure 9) but also on the inflatable structure of the cone (Figure 10). Moreover, the influence of the wall catalycity on the wall heat flux is more important for the Mars mission than for the Earth mission. Here, fully catalytic mechanism is expressed with a super-catalytic model assuming atomic recombination at wall at upstream levels for O_2 and N_2. This is chosen to size heating regarding the worst scenario for the wall thermal balance. Plasma jet tests planned later in the project will clarify actual catalycity for Hi-Nicalon outer fabric and allow deviation with sizing design conditions.

Material emissivity

Uncertainties exist on the value of the material emissivity which is essential to estimate the wall temperature through radiative cooling mechanism. The influence of the wall emissivity on the wall temperature is relatively small. Indeed, an error of 0.1 on the emissivity leads to a difference between 30 K and 50 K on the wall temperature according to the wall catalycity assumption. The scheduled test campaign will allow in particular to characterize the emissivity of the material and refine ATD results.

Citation: Guidotti G, Fuentes IP, Trovarelli F, et al. EFESTO - advancing European hypersonic inflatable heatshield technology for Earth recovery and Mars high-mass delivery missions. *Aeron Aero Open Access J.* 2022;6(2):59–73. DOI: 10.15406/aaoaj.2022.06.00142

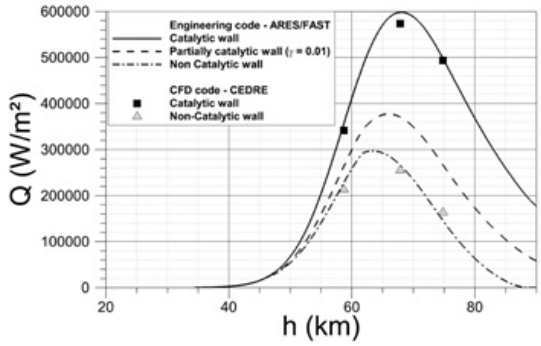

Figure 9 Influence of the wall catalysis on the stagnation point heat flux along the trajectory for the Earth mission.

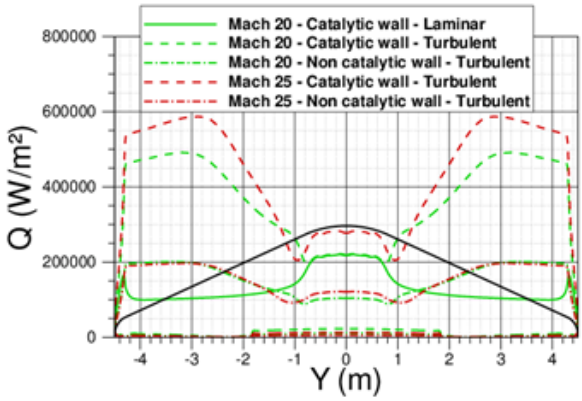

Figure 10 Influence of catalycity and laminar/turbulent boundary layer on the wall heat flux for the flight points [35 km, Mach 25] and [24 km, Mach 20] - CFD CEDRE simulations - Mars mission.

i. Turbulence on the blunt cone

Due to the inflatable structure enveloped with the flexible TPS material, the aerodynamic stresses encountered during atmospheric entry will likely induce a surface deformation: at the junction between the rigid nose and the flexible conical TPS, but also on the cone with emergence of surface scalloping. This has been highlighted by the IRVE-3 flight test.[19] As confirmed during the tests conducted at NASA Langley Mach 6 air tunnel[20] the deformed surface should promote boundary layer transition, leading to an important heating increase in the transition zone. Such boundary layer transition may be earlier triggered by the junction between the rigid and the flexible material or by undulating surface. Moreover, transition laminar-to-turbulent mechanism could occur at higher altitudes due to surface heterogeneity different from those driven by gap-and-step of reusable spacecraft or roughness from ablative material degradation. Preliminary simulations have been performed on a smooth geometry, where transition occurs at the junction between the sphere and the cone, to evaluate the turbulent heat flux on the conical part. For the Earth mission, the boundary layer stands laminar on the windward surface while on the leeside surface the effect of turbulence on the wall heat flux becomes significant from the flight point [Mach 17 – 65 km and 15° angle-of-attack]. Therefore, maximum heating remains located at stagnation zone. For the Mars mission, the turbulence mechanism leads to a major increase of the wall heat flux on a large part of the blunt cone (Figure 10). Indeed, the maximal heat flux on the cone is around twice the stagnation point value. Investigation of an undulating surface consequence on wall heat load has not been performed yet. According to[21] the flow expansion and compression induces flow separations and reattachments in the valleys in the leeward, leading to boundary layer transition. Peak heating is observed in the transition zone. However, the inflated structure here investigated is different from stacked torus structure depicted in literature (NASA in particular) since "annular tori" solution, has been preferred. Transition laminar-to-turbulent could evolve then in a different manner.

ii. Recirculation zone

According to the front-shield and the back-shield configuration, the shear layer could impact the rear payload wall during the re-attachment process, which could induce a peak heating that can reach 16% to 18% of the forebody stagnation point heat flux.[22] Therefore, investigated designs must prevent such mechanism to preserve payload integrity. Regardless of the configuration investigated, the shear layer never impacts the back of payload for Earth and Mars missions, as illustrated on Figure 11. The maximum heat fluxes recorded on the afterbody are less than 4% of the stagnation point heat flux (~ 3 kW/m² for Earth and ~13 kW/m² for Mars).

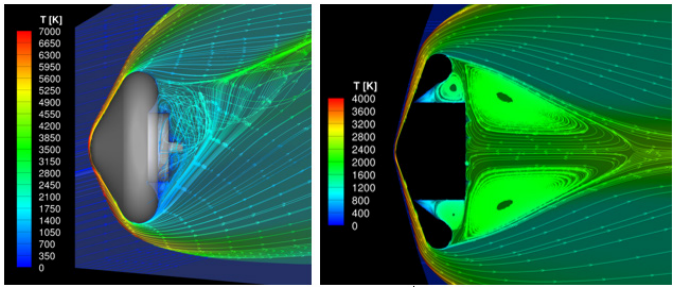

Figure 11 Visualization of the wake environment behind the HIAD - Earth and Mars design

Radiative heat flux

For the Mars mission, the radiative heat flux from the shock layer, received by the wall on the back-shield, could be non-negligible especially driven both by the significant size of the heatshield (8.8 m diameter) and high IR radiative intensity from CO and CO_2 molecules as predominant species in the shock layer. Maximum radiative heat loads are obtained for Mach 20 (Mach 25 being the peak convective-diffusive heating trajectory point) by using Monte-Carlo RHT solver ASTRE embedded in the CFD CEDRE code. Radiative over-heating process is then addressed and maximum levels of about 70 kW/m² and 20kW/m² respectively on front-shield and back-shield surfaces have been obtained and are taken into account to size the flexible TPS material. The radiative heat transfer level is independent on the both wall catalysis properties and turbulence assumption. This over-heating process is specific to the Mars Mission. For the Earth mission, radiative heating is assumed negligible with regards to the entry velocity (lower than 8.5 km/s) and the heatshield size (less than 5 m diameter). Indeed, IR or UV radiations intensity are limited in terms of shock layer high temperatures, shock layer volume size and air-species radiative power.

Margin strategy

Due to important uncertainties associated to the wall catalysis, the boundary layer transition and its influence on the wall heat flux, as well as, for the Mars mission, the effect of the radiative heat transfer, the following procedure has been applied to size the TPS material:

a) Super-catalytic heat flux is considered throughout the atmospheric entry;

b) Fully turbulent boundary layer from Peak heating point is recommended;

c) For Mars, sizing radiative heating levels have been added to convective-diffusive heating on the front and back shield;

d) On the back-shield, a minimum convective-diffusive heating value of 13 kW/m² is recommended.

Mission engineering and GNC

While the project focuses on the hypersonic and supersonic flight phases of the HIAD system, an end-to-end mission design has been performed by DEIMOS Space to achieve preliminary coherency of the overall solution in the CONOPS context defined in section I. Beyond reference trajectories, parametric mission analysis and trajectory simulations in worst cases have been performed to support the definition of the target ballistic coefficient and flight conditions. From these results, and in coordination with system design activities, specifications for the design of key subsystems have been derived, in particular the F-TPS (section VI) and the inflatable structure (section VII), and for the identification of testing conditions for plasma wind tunnel (section VIII) and IS ground tests (section IX). The design methodology relies on the company's experience and flight qualified tools successfully applied to missions like ESA's IXV[23] or ESA/Roscosmos' ExoMars16 Schiaparelli.[24] A synthesis of the results of the first steps of the design methodology are presented (reference mission and expected worst case performance) while the verification of the design (through Monte Carlo simulation and detailed assessment of margins to design constraints) is ongoing at the time of writing this paper and will be presented in a future paper. At GNC subsystem level, the concept design of the overall hardware elements and of the onboard software logics is ongoing to guarantee the proper execution of the sequence of flight mission phases, in particular for the controlled ones.

Earth application

After injecting its payload into the target orbit, the AVUM (VEGA upper stage) performs a deorbiting maneuver and burns up in Earth's atmosphere, demising in a safe area for ground population and unprotected by any TPS. This valuable hardware is lost at the end of each VEGA launch. The first key aspect considered in EFESTO is the need to protect the AVUM with a HIAD from the harsh entry environment and fly a feasible trajectory respecting the set of applicable requirements for the mission, in particular thermo-mechanical constraints during the most critical entry phase and that define the entry corridor (see Figure 12). The second key aspect considered is the possibility of recovering the AVUM at the end of the re-entry and with limited operations costs that justify the effort and the reusability of this hardware for reducing the overall cost of access to space. From a preliminary business case analysis, costs of operations should not exceed about 10% of the recovered hardware and at CONOPS level (see section I) this implies the minimum use of helicopters in the MAR operations. Having only one helicopter minimizes costs but imposes requirements on the landing accuracy of the system.

To reach the area within the helicopter range capability, three key needs have been identified (similar to the ESA's Space Rider, evolution of the IXV): an accurate deorbiting burn to limit dispersion at the EIP, a controlled entry and a controlled descent phase (under a parafoil). The controlled entry makes use of the aerodynamic lift (obtained by the aeroshape with an offset in the CoG location with respect to the symmetry axis, see section IV), and beyond enabling a control of the position of the vehicle, reduces the loads on the HIAD by gliding a longer and shallower trajectory when compared to a passive, ballistic entry, see Figure 13.

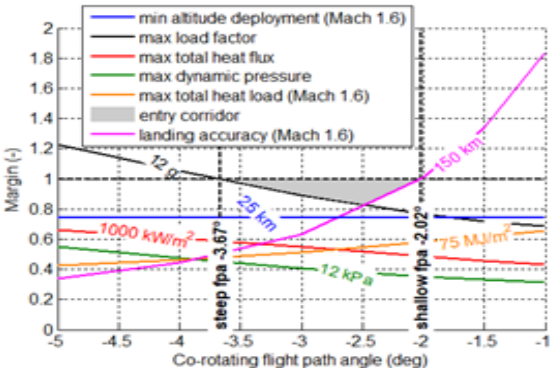

Figure 12 AVUM, entry corridor. Variability of trajectory margins with respect to constraints as a function of the flight path angle at the EIP.

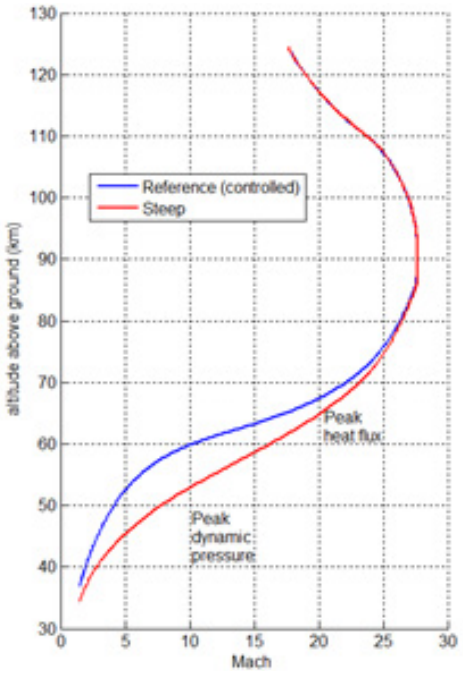

Figure 13 AVUM, sizing and reference (controlled) entry trajectories.

Mars application

For the Mars application, the baseline mission scenario selected foresees a direct entry from a hyperbolic arrival (Launch Window opportunity in the 2030-2040 timeframe explored) using a HIAD system (~9 m diameter, inflated before the EIP) to decelerate and protect the capsule in a ballistic entry phase and a SRP (Supersonic Retro-Propulsion) subsystem to slow down the 2500 kg payload from supersonic condition (Mach 2.3) to landing (target site located in Oudemans Crater, MOLA +2 km). Similar to the Earth scenario, reference and worst cases trajectories have been computed (Figure 14); the main differences are the fact that the capsule will perform a ballistic entry and that the control of the final target point is done with the SRP. For the SRP, 25 engines (Aerojet MR-80B, used in the skycrane landing phase of the Mars Science Laboratory mission) in ring configurations are considered, performing a controlled g-turn and a hovering at 20 m above ground, during which the payload is lowered to the surface of Mars (following the strategy adopted by NASA for of MSL and Mars 2020).

The trajectories obtained (Figure 15), designed in coordination with system and key subsystems (in particular HIAD and SRP),

demonstrate that it is possible to land a heavy scientific payload in regions of Mars never explored by any past or current mission to the planet. This goal is recognized as a challenging step in future exploration, and a necessary preliminary step for future human exploration of Mars and advances in TRL of both HIAD and SRP technology are needed to achieve it.

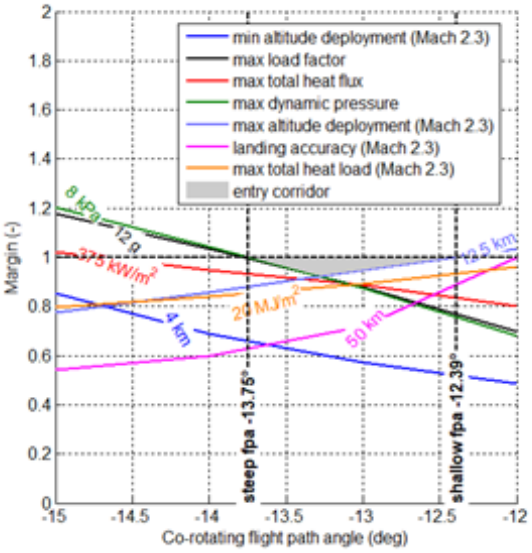

Figure 14 Mars, entry corridor. Variability of trajectory margins with respect to constraints as a function of the flight path angle at the EIP.

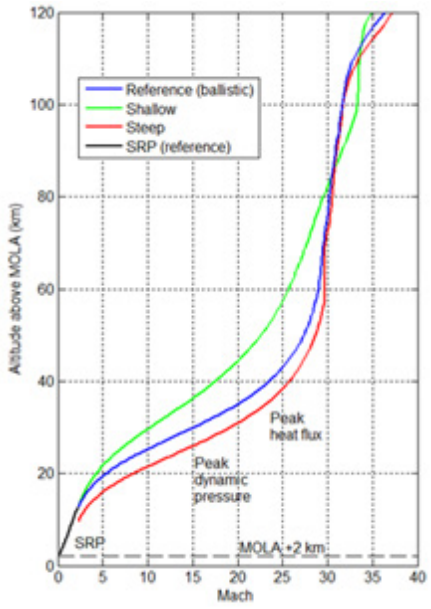

Figure 15 Mars, sizing and reference (ballistic) trajectories.

I. HIAD desig-n: flexible TPS

The F-TPS is a thin flexible multi-membrane structure that during the mission is in contact with the external environment: it is the main thermal protective element of the system.

This membrane must therefore simultaneously have many characteristics to achieve its goals:

a) the ability to withstand high temperatures (up to 1800ºC)

b) the ability to reject into the external environment most of the incident heat (up to 600kW/m2, see Figure 9)

c) the ability to not transmit heat to the structures to which it is connected or in direct contact

d) good mechanical characteristics, such as to withstand the pressure of the external "wind" and the tension imposed by the supporting structure,

e) Flexibility and foldability, to be able to pack in a small space and then return to the ideal shape without opposing particular resistance.

The real possibility of making such a membrane and its final performance (weight and size) depends on the characteristics of the materials used. There is no material able to fully satisfy, on its own, all the requirements listed above: therefore, a mix of different materials must be integrated to obtain a very efficient membrane. In general, these types of membranes consist of the superposition of several different layers of fabric, each with different characteristics depending on its position in the stack. Typically, F-TPS are multi-layer structures where the outer layer, the one that interacts with the external environment, it's exposed to the highest temperature, and the inner layers are built to prevent the diffusion of heat in order to isolate and protect the internal structures of the system.

The first part of this study was therefore based on the search for materials that had interesting characteristics for the realization of this project. Attention was focused on all those fabrics, mats, foams with thermal insulating capabilities.

A rich database of dozens of materials was collected: for each material, in addition to the classic thermal and structural characteristics (for example thermal conductivity, maximum operating temperature, density, resistance to breakage, etc.) the different types of yarn produced (based on the weaving of the fibers), the thicknesses and formats of the available mats or rolls, since this decisively affects the possibility of making the final membrane, its bending and folding capability, the number of joints needed to cover all the designed area, and ultimately the overall reliability of all the multi-layered structures have been evaluated. The cost of the materials and their availability for the European market were also considered.

A FEM simulation environment was developed to carry out thermal analyses to test, compare and choose between the different membrane configurations. The behavior of one or more elementary pieces of F-TPS was simulated, that is, portions of membrane with real thickness but a unitary plan area (for example 1 mm2). These blocks where chosen between the most significant points of the membrane (e.g. on the cone or the tip of the F-TSP, see Figure 16) and on the basis of opportunity criteria, generally the most critical points for heat flow or on transition zones. In this thermal model, the incident thermal flux is applied to the external surface as a function of the time of the mission (data are provided by the fluid dynamic analyses of the mission). Figure 17 shows the temperature map simulated on a sample of F-TPS multilayered structure (Mars application) at mission time = 150s. For each simulated sample, the calculated data were:

a) maximum temperature reached for each layer (needed to verify feasibility)

b) maximum temperature at the interfaces with adjacent structures (e.g. in a critical point where the maximum temperature is limited by the characteristics of the material used to build the structure itself)

c) thickness and density, to evaluate the volume and mass efficiency of that specific configuration.

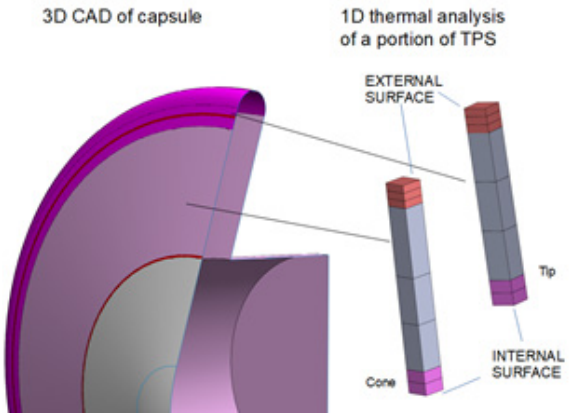

Figure 16 Thermal simulation methodology.

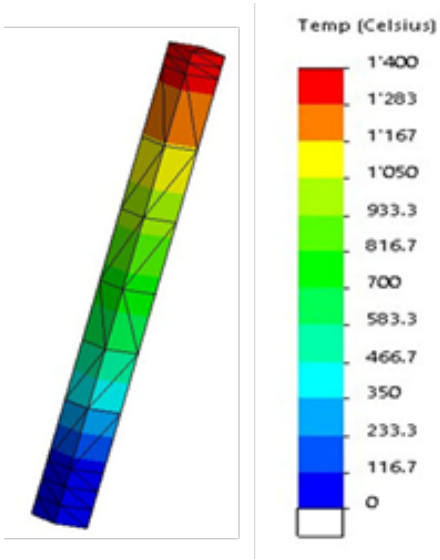

Figure 17 FEM analysis on F-TPS stack, temperature map at mission time = 150s.

The solver works with the characteristics of the individual layers (type of material, thermal resistance contact and thickness) provided by the database collected. A trade-off analysis was carried out leading the FEM simulation of several different configurations, both for the Earth mission and Mars mission scenarios. The parameters to evaluate and choose among the F-TPS options have been defined for performance, foldability, manufacturing, and procurement properties of the layers. Applying the Analytically Hierarchical Process (AHP) method the parameters, or criteria, are weighted through pairwise comparison. The whole consortium has been involved in the weighting process and hence in the definition of the influence of each criterion in the final ranking. Additionally, the possible F-TPS layers configurations have been filtered for feasibility, and according to upper bounds for the thickness and the density of the layers. A sensitivity analysis has been performed for the resulting ranking showing a good robustness of the result. The same trade-off methodology has been used for both the Earth and the Mars scenario, for which different criteria weights have been considered for the two mission scenarios. For example, in the Mars scenario the weight of "density" influences more the final ranking respect to other parameters, as "stowed envelope", "foldability" or "cost".

This extensive screening shows that several solutions are feasible and some of these are close each other if we consider only the trade-off results. Additional considerations, carried out at system level, made it possible to choose a reference configuration that fulfills all the requirements. The final design, for both Earth and Mars scenario, is a multi-layer and multi-material configuration similar to a symmetric "sandwich". From this reference configuration, optimized for the worst heat flux conditions of each mission (worst in space and time), we derived other multi-layer and multi-material configurations, with reduced mass, thickness and stowed volume, able to protect the area of system where the heat fluxes are lower.

The final F-TPS used to protect the whole system during the re-entry phase of the mission is made by a multi-layer rigid and flexible membrane with different thicknesses, optimized for each different area. This approach guarantees to meet the requirements and at the same time reduce the mass and the stowed volume (Figure 18).

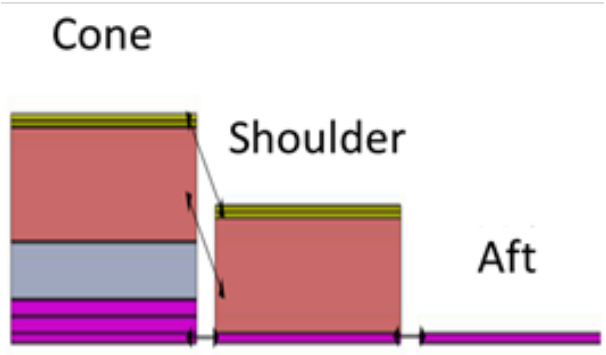

Figure 18 Final F-TPS structure.

II. HIAD design: inflatable structure

The evolution of the design for the inflatable structure started considering the first concepts studied in literature like the "Tension cone" configuration (see Figure 19), which has great advantages like:

a) has high realization simplicity;

b) has high simplicity in the defining the deceleration drag "footprint";

c) produce high drag;

d) is able to align its geometry to the vehicle flight path.

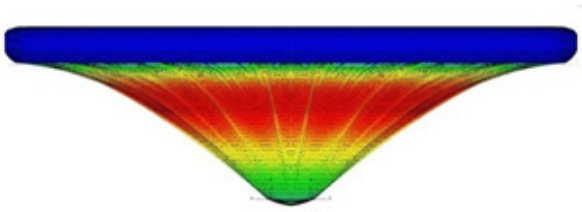

Figure 19 Tension cone.

However, some issues determine the abandonment of this solution. Those issues are mainly linked to "cupping" and wrinkling phenomenon of the fabric cone, and the adding of a burble fence to the structure did not yield significant improved dynamic stability. Furthermore, the single inflatable torus configuration suffers of unpredictable behavior of the structure, buckling and twisting out of plane, under external loads.

The second chosen configuration is the "Stacked Torus IAD" configuration, which solves the main problems of the previous solution:

Citation: Guidotti G, Fuentes IP, Trovarelli F, et al. EFESTO - advancing European hypersonic inflatable heatshield technology for Earth recovery and Mars high-mass delivery missions. *Aeron Aero Open Access J.* 2022;6(2):59–73. DOI: 10.15406/aaoaj.2022.06.00142

a) the buckling of the single torus is partially solved by stacking a family of concentric and interconnected tori

b) cupping is eliminated by the new configuration itself, providing a structural conic substrate.

The Stacked Torus IADS architecture developed by NASA Langley Research Center (LaRC) comprises a conic assembly of inflatable circular air beams as schematically shown in Figure 20. This design, originally implemented since 2004 in NASA's Inflatable Re-entry Vehicle Experiment (IRVE) program, is widely documented in the literature[25–27]

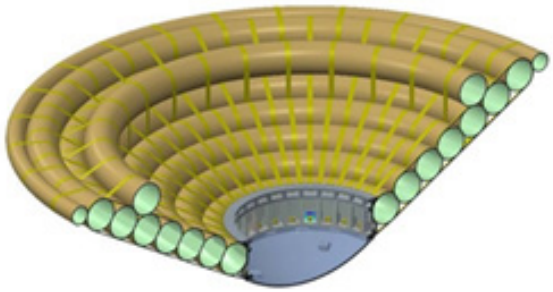

Figure 20 Stacked torus.

However, this configuration led to some problems like:

a) non-scalability: the global sphere cone design is, at best poorly scalable (rationale in the text below)

b) structural indeterminacy linked to the braided air beam construction, the amount of mass needed to knock-down factor associated to this indeterminacy and the structural capability itself linked to the interaction between different geometries (multiple tori)

c) high cost due to the extensive validation effort and manufacturing complexity

As far as scalability is concerned, the air-beam torus is very poorly scalable. Each increase in size and pressure becomes a point design requiring different braid parameters and, therefore, a renewed fabrication protocol and validation program. The main reason is the innate predisposition of toroidal structures to buckling failure as extensively documented in.[27] Body flex and off-axis performance is poor: individual tori present limited out-of-plane stiffness, requiring a complex (and difficult to characterize) network of interconnecting straps to stabilise the toroidal stack.

In addition, a general vulnerability of fiber misalignment in high specific strength air-beam braids is also a constant issue a seen in an IRVE torus pressure restraint (Figure 20). While low elongation and high modulus of high performance fibers is a great benefit for maintaining vessel geometry, it quickly becomes an Achilles' heel if the vessel is not meticulously engineered.

Due to their high modulus, it is difficult to guarantee proper load sharing between individual fibres within a braided "acreage" (large area coverage) product, thereby making any discontinuity susceptible to point load induced failure. This does not ultimately bode well for these 'broad coverage' fiber constructs since, the greater the area of pressurized coverage, the more difficult it becomes to precisely balance the load sharing between individual fibres.

Fiber misalignment in high specific strength braids and weaves is a perpetual concern as source of point-load structural failure, and at very least, a perpetual source of stress distribution uncertainty due to manifestation of indeterminate load pathways.

As shown in Figure 20, the general vulnerability of fiber misalignment in high specific strength air-beam braids, seen here in an IRVE torus pressure restraint. While low elongation and high modulus of high performance fibers is a great benefit for maintaining vessel geometry, it quickly becomes an Achilles' heel if the vessel is not meticulously engineered. Due to their high modulus it is difficult to guarantee proper load sharing between individual fibres within a braided "acreage" (large area coverage) product, thereby making any discontinuity susceptible to point load induced failure. This does not ultimately bode well for these 'broad coverage' fiber constructs since, the greater the area of pressurized coverage, the more difficult it becomes to precisely balance the load sharing between individual fibres. Fiber misalignment in high specific strength braids and weaves is a perpetual concern as source of point-load structural failure, and at very least, a perpetual source of stress distribution uncertainty due to manifestation of indeterminate load pathways.

As shown in Figure 21, the hand application of adhesive to a NASA IRVE torus "locks" the high modulus restraint fibers in place to preclude further fiber misalignment, particularly during packaging, transport, and deployment. The adhesive is also critically important to bond the internal gas bladder to the inner surface of the pressure restraint. However, failed local bonding between restraint and bladder can lead to "bridging" of the bladder, then potentially leading to bladder rupture. This assembly process is extremely laborious, difficult to ensure reproducibility, and fraught with potential performance indeterminacy.

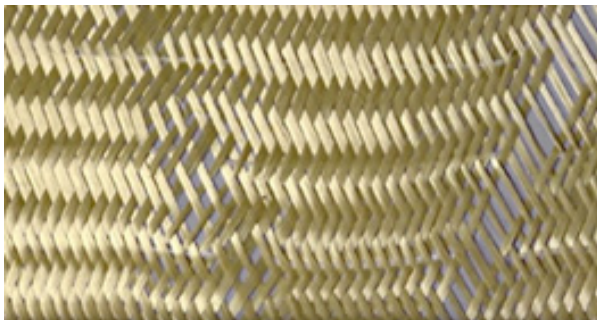

Figure 21 NASA torus braid misalignment.

Furthermore, the torus configuration presents high inflation gas leakage potential due to high inflation pressure requirements, extensive seam lengths, and high surface to volume ratio. The aeroshell's flight regime for a HIAD mission begins with exoatmospheric inflation. The loads acting on the inflatable structure come from internal inflation pressure and from the dynamic pressure of re-entry and associated deceleration. The Inflatable Structure (IS) is required to provide sufficient rigidity and stiffness to maintain its intended decelerative performance throughout re-entry, whereby inflation pressure is minimized to reduce the mass fraction for the inflation system. The lowest acceptable pressure will furthermore be associated with prescribed geometry and sufficient material tautness to preclude heating in excess of the temperature tolerances of fabrication materials (Figure 22).

In order to overcome the development challenges of the NASA configuration, the "Annular Torus" configuration has been proposed in the current project (Figure 23), derived by the UHPV (Ultra High-Performance Vessel) pressure vessel architecture developed by Thin Red Line.[28]

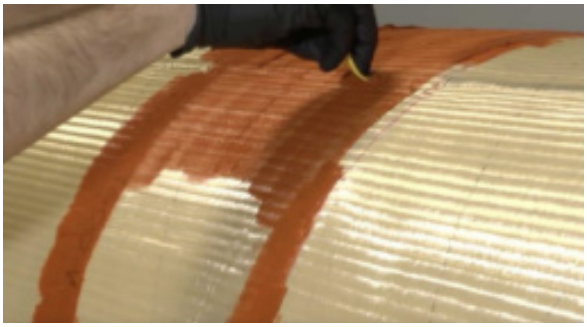

Figure 22 NASA torus adhesive application.

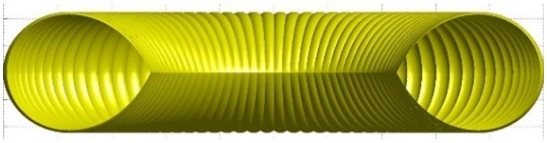

Figure 23 Annular torus.

This configuration solves many of the problems of the Stacked tori configuration:

a) it has the highest specific strength (strength-to-mass ratio) with respect of other competing design.

b) it has structural determinism, with exceptional performance predictability.

c) it is scalable.

The most straightforward implementation of Annular Tori based configuration is to replace each of the conventional Air Beam Tori of NASA's HIAD configuration with the Annular Torus counterpart. In general, two drawbacks are associated with both the stacked torus and the similar "stacked Annulus" configurations:

a) high aperture sphere cone configurations (like the 70-degree for the Mars application) are much more challenging to structurally define than 60- and 45- degree sphere cones.

b) the TPS "scallops/indents" between the tori (or annuli), introducing an increased mechanical load and a more complex predictive model for the aero heating.

For this reason, the Stacked Annulus configuration has been discharged and instead another implementation of Annular Tori has been adopted for both the Earth and Mars scenario with two slightly different configuration optimized for each scenario.

Earth application

For the Earth scenario the adopted solution is based on two separate inflatable volumes. The first one shown in light grey in Figure 24 is the Annular Torus.

The main task of this inflatable structure is to sustain the main loads along the trajectory. The second volume depicted in dark grey in Figure 24 is a secondary conical volume with the function to maintain the external shape during re-entry and with the advantage compared to the stacked torus configuration of avoiding TPS scallops between the tori.

This configuration compared to the "Stacked Torus" is less complex and can be considered as an evolution of the "Tension Cone" configuration, avoiding in the same time the problem of buckling and cupping that affected that solution.

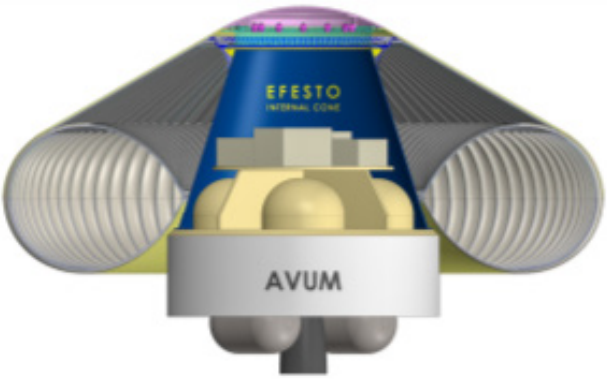

Figure 24 Inflatable structure earth configurations.

Mars application

The diameter of the inflatable structure for the Mars scenario is twice the size compared to the one developed for the Earth scenario. Adopting the exactly same configuration used in the previous paragraph would lead to a much bigger and heavier structure. For this reason, some modifications have been introduced.

First of all, also in this configuration the same two separate inflatable volumes have been maintained and respectively an Annulus Torus and a Conical Volume. The main difference is that in this case the Annular Torus in not directly in contact with the main body to avoid an excessive size of the Annular Torus as in Figure 25. Also, in this configuration the conical volume is used to maintain the desired shape along the re-entry trajectory. The two inflatable volumes have different values of pressurization for each configuration that have been designed ad-hoc for the reference missions.

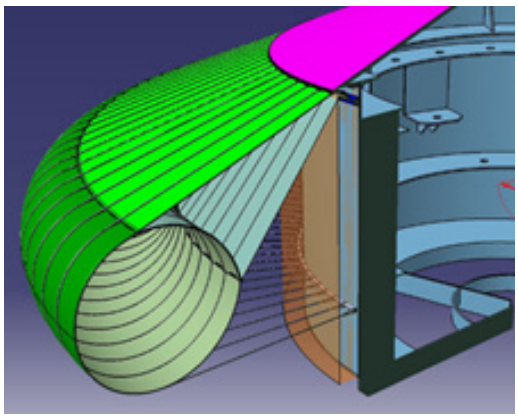

Figure 25 Inflatable structure mars configuration.

I. Ground tests campaigns: plasma wind tunnel

The development of the proposed inflatable TPS solutions will be supported by thermal characterization in ground test facilities. Two test campaigns are foreseen in DLR's arc-heated facilities LBK. In the first arc-jet loop, selected candidate TPS designs will comparatively be tested on sample basis at mission relevant conditions. The candidates are being identified during the detailed HIAD design. The results of the arc-jet tests will support the selection of the most suitable TPS layups for both applications, Mars as well as Earth. The second arc-jet loop will then be objected to the final TPS design. Beyond the flexible TPS membrane, the specimens for this series of tests will also include elements of the inflatable structure.

Thermal qualification of TPS materials and structures for atmospheric entry missions require test conditions

a) at flight relevant enthalpy conditions and

b) in realistic thermochemical environment.

Such conditions can be achieved in arc-heated facilities operating in supersonic or hypersonic mode, as e.g. the LBK facilities. LBK consists of two individual test legs, named L2K and L3K. A principal sketch of the facility is shown in Figure 26. Each test leg is set up similar to a conventional hypersonic blow-down wind tunnel, complemented, however, by an arc-heater to energize the working gas to high enthalpy conditions. L3K is equipped with a segmented arc heater with a maximum electrical power of 6 MW, L2K uses a 1.4 MW Huels-type arc-heater.

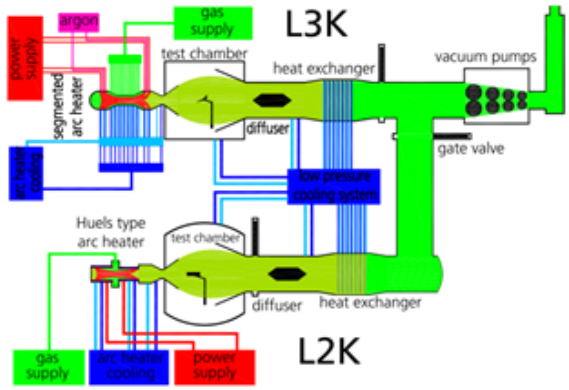

Figure 26 DLR's arc-heated facilities LBK.

For thermal testing, samples and models are placed in the homogeneous hypersonic free stream, which is generated by a convergent-divergent nozzle. The nozzle is modular, its expansion part is conical with a half angle of 12°. Different throat diameters from 14 mm to 29 mm are available and can be combined with nozzle exit diameters of 50 mm, 100 mm, 200 mm, and 300 mm. So, the facility setup can effectively be adapted to particular necessities of a certain test campaign. This particular mode of operation allows for testing in a realistic chemical environment at free stream Mach numbers between 4 and 10. A more detailed description of the facility is given by Gülhan et al.[29,30]

The L2K facility can be used to perform tests in Martian atmosphere, by using a mixture of 97% CO_2 and 3% N_2 as working gas. Accordingly, the tests related to the Mars application are planned for L2K, while the TPS of the Earth application will be characterized in the L3K facility.

Both arc-jet loops will include tests in stagnation configuration and in wedge configuration. Stagnation tests are required to characterize the TPS layups' principle capabilities in sustaining a high-enthalpy environment specified by atmosphere, heat flux and stagnation pressure. Due to the low number of testing parameters, the results of stagnation tests are also well suited for the validation of simulation models. The wedge configuration, however, is closer to application, since the aerothermodynamic loading includes shear loads applied by the flow.

Thermal tests on flexible TPS samples require particular sample holders. During their initial PAIDAE program, NASA embedded several flexible layups into silica tiles for concurrent comparative testing in shear flow configuration in the 8ft high temperature tunnel at LaRC.[31] In the frame of the HIAD program an improved test setup, which allowed for setting a specific tension on the external fabrics, was applied for shear flow testing at the Boeing LCAT facility.[32] Two model holders were designed for tests on flexible layups in stagnation configuration, one with a ceramic, the other with a metallic water-cooled framework. Basing on the ceramic stagnation holder of NASA, a stagnation holder was designed at DLR. Geometry was particularly adapted to the characteristic dimensions of the L2K facility. First application with flexible layups was realized in the frame of ESA's study "Aerothermodynamics Tools for Inflatable Hypersonic Decelerators."[33]

A principal sketch of the stagnation holder is shown in Figure 27. The model holder has an external diameter of 70 mm. On its front surface it provides an open diameter of 45 mm for the flexible sample, which may consist of several layers of fabrics, insulation and gas barriers with a total thickness of to 30 mm. The fabrics form the external layer. They are held in tension by a clamped jacket. Insulation layers and potential gas barrier layers can be installed from the back. Between these layers, thermocouples can be placed to take temperature measurements inside the TPS layup. In addition, the surface temperature can be measured non-intrusively by infrared instruments, as e.g. pyrometers. Figure 28 shows a photograph of the complete stagnation test assembly.[34]

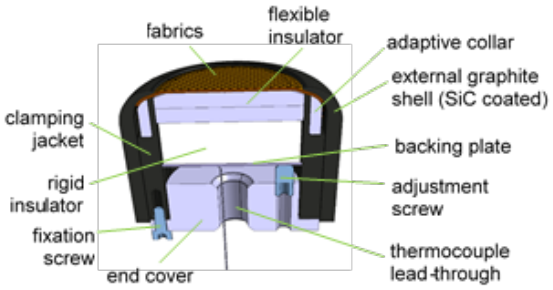

Figure 27 Stagnation holder for flexible TPS.

Figure 28 Stagnation test assembly.

For the tests in wedge configuration, an existing flat plate model holder will be modified for the integration of flexible TPS samples. A square area of 70 mm by 70 mm will be exposed to the flow. Also, for this setup, special care will be given to keep the external fabric layers in tension during the tests.

The test conditions are derived from the trajectory data of the two applications, with particular consideration of maximal heat flux and maximal dynamic pressure conditions. Two different test conditions will be defined for each application. The test durations will consider the projected integral heat loads. For all test conditions and configurations, repeatability tests are included to improve the reliability status of measured data.

Additional support to aerothermodynamic modelling in EFESTO will be provided by material characterization. For the materials included in the candidate flexible TPS layups, the most decisive thermal properties will be measured by standard laboratory techniques according to common standards, covering the complete temperature

range from ambient temperature up to the expected maximal temperatures of the reference missions.[35]

II. Ground tests campaigns: inflatable structure

As per the Flexible TPS materials, multiple aspects will be covered on inflatable structures by test allowing: research on materials, ground demonstration tests, models validation and extrapolation to flight. Two parallel activities will be carried out as follows:

Test at material assembly level

Knowledge of mechanical properties of the Inflatable Structure is fundamental for simulation of structural performance during packing, inflation and deployment. Therefore, investigation of mechanical behavior of IS layers will be appointed through manufacturing and testing of various samples at raw/semi-finished level.

Tensile tests warp/weft on structural fabric and webbing samples will cover: biaxial tensile, puncture, abrasion resistance, bonding\welding\stitched joint strength, ageing, permeability. This type of characterization will be applied also for TPS materials which usually are lacking about mechanical properties characterization.[36]

Ground demonstration tests

The ground demonstration tests campaign aims at reaching TRL 4 for inflatable structures.

Investigation of mechanical behavior of Inflatable Structure as a sub-system will be achieved through design, manufacturing and testing of a 1:2 Demonstrator (2.4 m diameter) with particular focus on key aspects as folding and stowing, inflation process and capability to withstand static load patterns (see Figure 29).

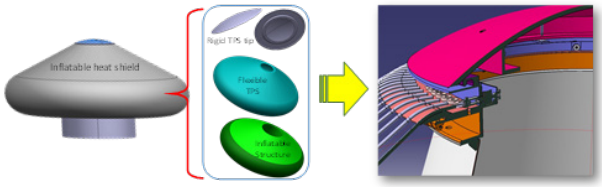

Figure 29 EFESTO 1:2 Ground Demonstrator – CAD model.

The Demonstrator will replicate 1:1 the Inflatable structure architecture, materials and design solution. On the contrary, a simulacrum of the F-TPS skirt will be manufactured to replicate packing density and mechanical strength see Figure 30.

Figure 30 EFESTO 1:2 Ground demonstrator – simulacra of the F-TPS.

Two specific dedicated tests will be carried out:

a) Inflation and Deployment Test: to provide a feedback about critical aspects as folding and packing method, inflation phase and deployment sequence see Figure 31.

b) Static Load Test: to characterize the structural deformation of IAD model under a symmetrical and asymmetrical load distribution see Figure 32.

As far as the Inflation and Deployment test is concerned, the test philosophy is a replication of representative inflation using compressed air at equivalent design inflation pressures (with the system at ground conditions). The stowing process will be appointed first by wrapping around the Inflatable Structure in its "deflated" configuration. Also, some auxiliary belts and a confinement bell will be used and then removed to simulate the deployment. Afterwards, the inflation will be executed to let the morphing process to take place. A video footage of the whole test session will be carried out in order to allow for later observation of the process.[37]

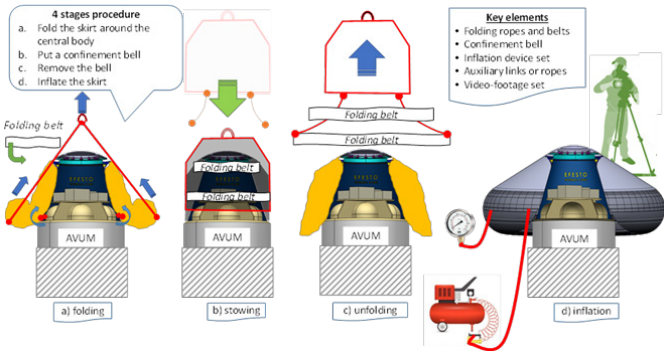

Figure 31 EFESTO Ground demonstrator – Inflation and Deployment test.

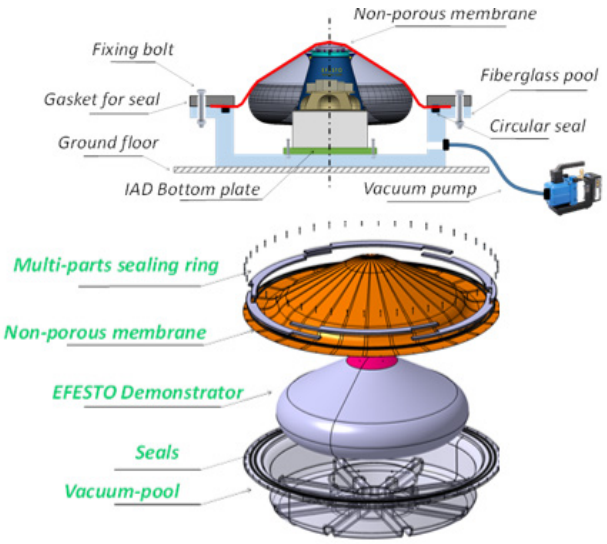

Figure 32 EFESTO Ground demonstrator– Static Load test.

As far as the Static Load test is concerned, the test philosophy is a replication of the sizing entry condition (max dynamic pressure) by application of an equivalent static load pattern. To do so, a distributed load pattern on the external conical surface of the Inflatable Structure will be realized through vacuum on a complex ad-hoc test rig. In order to allow proper execution of this particular test, an ad-hoc test-rig is being designed and manufactured, the peculiarity being the non-porous membrane that will allow for the static pressure to stand against the conical surface of the Inflatable Shell of the Demonstrator. The vacuum environment will be set-up during the test execution thanks to adoption of a particular sealing solution along with a vacuum pump.

The 1:2 Ground Demonstrator will be equipped with a set of load-cells to measure the forces standing at the tendons level. A COTS acquisition and transmission solution will be adopted in 8 load cells each one equipped with a wifi transmitter. All the sensors signals will be acquired by a dedicated device on a laptop for data monitoring and processing. A video-footage system will be exploited based on CIRA heritage and hardware of high-speed phenomena as crash-testing of aircraft.

Citation: Guidotti G, Fuentes IP, Trovarelli F, et al. EFESTO - advancing European hypersonic inflatable heatshield technology for Earth recovery and Mars high-mass delivery missions. *Aeron Aero Open Access J.* 2022;6(2):59–73. DOI: 10.15406/aaoaj.2022.06.00142

The IAD testing campaign will be carried out with exploitation of many hardware and items, some to be designed and manufactured, some other to be procured. In particular the following will be adopted: MGSE to support the Test Article, Winch or crane to trigger unfolding, Video-footage system, Sensors acquisition system, Hoisting system, Air-compressor system.

III. Technology roadmap and way forward

The EFESTO project aims in developing technologies enabling space exploration missions requiring payloads delivered, to celestial bodies with an atmosphere, larger than current launchers size limits or to not yet accessible landing locations. Moreover, the EFESTO system may be used in enhancing the reusability of access to space vehicles.[38]

A technology roadmap will place the project in the worldwide context suggesting the step by step development for the European effort in the field. A road mapping methodology based on the POLITO heritage is used. The methodology includes stakeholder analysis, elements identification, prioritisation of the potential scenarios and technologies, planning definition, roadmap analysis.

At this stage of the project, the Consortium had identified and characterise the elements involved for the development of an inflatable aerodynamic decelerator (IAD). These will serve to the generation of the technology roadmap. Among the main operational capabilities (high-level functions) to enable, the launcher's upper stage reusability and the capability to land up to 2.5 tons at MOLA +2 km stands out respectively for the Earth and the Mars application. A relatively large number of relevant technologies have been identified (more than 25), and the technology groups most related to the project and the operational capabilities identified are (according to the ESA Technology Tree[26]):

a) Structural Material Concepts

b) Joining Technologies For Inflatable and Deployable Structures

c) New Advanced Hot Structures Materials

d) Landing Attenuation Technologies

e) Reusable Subsystems

f) Coatings and Insulation

g) Thermal Analysis of Materials

In particular, the project focuses on the development of flexible structural and TPS material.

During the development, some system and performance parameters are considered to evaluate the state of the development. The main are identified as: the decelerated payload, the inflatable system stowing and deploying properties, the F-TPS performances. These parameters are used during the trade-off analyses to choose among different scenarios and concept evolutions.[39]

A survey of space missions and programmes in the same technology domains has been performed. A timeline spanning from 1996 to 2025 has been populated with the data retrieved (more than 70 relevant programmes). The number and distribution of such programmes in the timeline is proof of the common interest and need in developing the aerodynamic decelerator technologies.

Among the future programmes, it is worth mentioning LOFTID by ULA and NASA, that will demonstrate second-generation F-TPS materials and higher diameters (6 m) of the inflatable decelerators.[1] The LOFTID system is the most similar to the EFESTO concept, it may be considered its European analogue.

So far, NASA's HIAD IRVE programme demonstrated the feasibility of the inflatable spacecraft technology with the stacked torus design and a diameter up to 3.5 m. The EFESTO annulus concept is the present moment of the inflatable technology development, where the arc-jet tests together with the structural models will provide breakthrough knowledge for future IOD missions.[40]

The activities mentioned above will enable larger inflatable aerodynamic decelerators and hence they will increase the space exploration capabilities (Figure 33). Moreover, the EFESTO project outcomes may serve not only to the missions mentioned, i.e. the Earth and Mars application, but it could be studied also for integration to future space exploration missions involving other planets or natural satellites.

The Technology Readiness Level (TRL) of materials yet under development is monitored as for the potential integration in the further development of the IAD concept and its configurations.

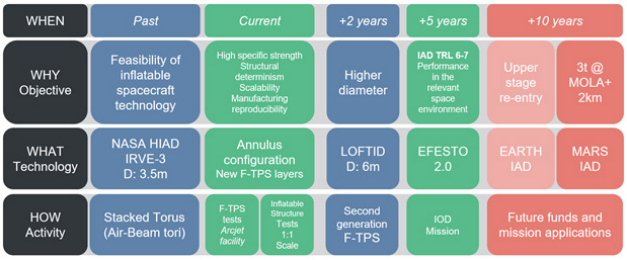

Figure 33 High-level preliminary EFESTO roadmap.

Conclusion

A general overview of the EFESTO project lines of activity has been given. Key results regarding the applications of inflatable aerodynamic decelerators for Earth and Mars have been presented, in the disciplines of system design, aerodynamics, aerothermodynamics, flying qualities, mission analysis and GNC. An overview of both the F-TPS and the inflatable structure design has been presented, together with the current plan of testing activities that are under preparation within the overall goal of comparing numerical predictions with experimental results. This step is recognized as fundamental and necessary at European level and is put in the overall context of the technology roadmap identified to increase the current European TRL and mature the knowledge in inflatable heat shields towards future real applications. Ambitious missions such as advanced Mars exploration or launchers upper stages reusability could significantly benefit from this technology.

Given that the focus of the EFESTO project is on the inflatable structure and flexible TPS disciplines, further work is recognized to be necessary for a fully coherent system design. In particular, stronger synergies with a design launcher authority on upper stage design and business case analysis are a desirable next step and as well as a coordinated technology development in parallel enabling technology (such as SRP on Mars or controlled parafoil flight and MAR on Earth).

Appendix

More information available at: http://www.efesto-project.eu

Acknowledgments

The EFESTO consortium acknowledges essential contributions of TRLA Aerospace Canada and ALI Scarl Italia.

Conflicts of interest

The author declares that there is no conflict of interest.

Funding

This project has received funding from the European Union's Horizon 2020 research and innovation programme under grant agreement No 821801. More information available at https://cordis.europa.eu/project/id/821801.

References

1. Dillman RA, DiNonno JM, Bodkin RJ, et al. Planned Orbital Flight Test of a 6m HIAD. 15th International Planetary Probe Workshop. 2018.
2. Marraffa L, Boutamine D, Langlois S, et al. IRDT 2R mission first results. Proceedings 5th European Workshop on Thermal Protection Systems and Hot Structures; Noordwijk, The Netherlands; 2006.
3. Hughes S, Dillman R, Starr B, et al. Inflatable Re-entry Vehicle Experiment (IRVE) Design Overview. American Institute of Aeronautics and Astronautics.
4. Chen T, Moholt M, Hudson L. Hypersonic Inflatable Aerodynamic Decelerator (HIAD) Torus Mechanical Testing. NASA Armstrong Flight Research Center; Edwards, California.
5. Reed J, Ragab M, Cheatwood M, et al. Performance Efficient Launch Vehicle Recovery and Reuse. *American Institute of Aeronautics and Astronautics*. 2016.
6. Vega User's Manual. *Arianespace*. 2014;4(0).
7. In-Space Propulsion Data Sheets, Monopropellant and Bipropellant Engines. *Aerojet Rocketdyne*. 2019.
8. Prévereaud Y. Contribution to the modeling of the atmospheric re-entry of space debris. Doctoral thesis. University of Toulouse, France; 2014.
9. Annaloro J, Galera S, Kärräng P, et al. Space debris atmospheric entry prediction with spacecraft-oriented tools. 7th European Conference on Space Debris; Darmstadt, Germany; 2017.
10. Refloch A, Courbet B, Murrone A, et al. CEDRE Software. *ONERA Aerospace Lab Journal*. 2011.
11. Sutton K, Graves RA Jr. A General Stagnation-Point Convective Heating Equation for Arbitrary Gas Mixtures. *NASA TR.* 1971;376.
12. Fay JA, Riddell FR. Theory of Stagnation Point Heat Transfer in Dissociated Air. *Journal of the Aeronautical Sciences*. 1958;25(2):73–85.
13. Sagnier P, Vérant JL. Flow Characterization in the ONERA F4 high enthalpy wind tunnel. *AIAA Journal*. 1998;36(4):522–531.
14. Prévereaud Y, Vérant JL, Balat-Pichelin M, et al. Numerical and experimental study of the thermal degradation process during the atmospheric re-entry of a TiAl6V4 tank. *Acta Astronautica*. 2016;122:258–286.
15. Bird GA. Molecular Gas Dynamics and the Direct Simulation of Gas Flows. *Oxford Engineering Science Series*.1994;42.
16. Owens RV. Aerodynamic Characteristics of Spherically Blunted Cones at Mach Numbers from 0.5 to 5.0. *NASA Technical Note*. 1965.
17. Calloway RL, White NH. Measured and Predicted Shock Shapes and Aerodynamics Coefficients for Blunted Cones at Incidence in Air at Mach 5.9. *NASA.* 1980;1652.
18. Edquist KT, Desai PN, Schoenenberger M. Aerodynamics for the Mars Phoenix Entry Capsule. *Journal of Spacecraft and Rockets.* 2011;48(5):713–726.
19. Olds AD, Beck RE, Bose DM, et al. IRVE-3 post-flight reconstruction. *AIAA Aerodynamic Decelerator Systems Conference* 2013;25–28.
20. Hollis BR, Hollingsworth KE. Surface heating and boundary-layer transition on a hypersonic inflatable aerodynamic decelerator. *Journal of Spacecraft Rocket*. 2018;55(4):1–21.
21. Zhao Y, Yan C, Liu H, et al. Assessment of laminar-turbulent transition models for Hypersonic Inflatable Aerodynamic Decelerator aeroshell in convection heat transfer. *International Journal of Heat and Mass Transfer*. 2019;132:825–836.
22. Horvath T, Hannemann K. Blunt body near-wake flow field at Mach 10. *35th AIAA Aerospace Sciences Meeting & Exhibit*. 1997.
23. Bonetti D, De Zaiacomo G, Blanco Arnao G, et al. IXV Mission Analysis Post Flight. *8th European Conference for Aeronautics and Space Science*. 2019.
24. Bonetti Bonetti D, De Zaiacomo G, Blanco Arnao G, et al. ExoMars 2016: Schiaparelli coasting, entry and descent post flight mission analysis. *Acta Astronautica*. 2018;149:93–105.
25. Hughes S, Dillman R, Starr B, et al. Inflatable Re-entry Vehicle Experiment (IRVE) Design Overview. 18th AIAA Aerodynamic Decelerator Systems Technology Conference and Seminar. 2005;1636.
26. Westman J. ESA Technology Tree. 2020;4.
27. Weaks GE. Buckling of a pressurized toroidal ring under uniform external loading. *NASA Tehnical note.* 1967;4124.
28. de Jong M. Flexible Vessel. US8186625. 2012.
29. Gülhan A, Esser B. Arc-Heated Facilities as a Tool to Study Aerothermodynamic Problems of Reentry vehicles, Advanced Hypersonic Test Facilities. *Progress in Astronautics and Aeronautics*.2002;198:375–403.
30. Gülhan A, Esser B, Koch U, et al. Mars Entry Simulation in the Arc heated Facility L2K. Proceedings of the 4th European Symposium on Aerothermodynamics for Space Vehicles. 2001;487:665–671.
31. Hughes S, Ware J, DelCorso J, et al. Deployable Aeroshell Flexible Thermal Protection System Testing. *American Institute of Aeronautics and Astronautics*. 2009.
32. Bruce W, Mesick N, Ferlemann P, et al. Aerothermal Ground Testing of Flexible Thermal Protection Systems for Hypersonic Inflatable Aerodynamic Decelerators. *9th Int. Planetary Probe Workshop*. 2012;16–22.
33. Johnstone E, Esser B, Gülhan A, et al. Investigating the Response of a Flexible TPS to a High Enthalpy Environment. *Int. Conference on Flight Vehicles, Aerothermodynamics and Re-entry Missions & Engineering*. 2019.
34. Keith R, Johnson F McNeil, Cheatwood, et al. HIAD Advancements and Extension of Mission Applications. *13th International Planetary Probe Workshop*. 2016.
35. Kazemba D, Cassell AM, Kushner LK, et al. Determination of the Deformed Structural Shape of HIADs from Photogrammetric Wind Tunnel Data. *Aerodynamic Decelerator Systems Technology Conferences*. 2013;1286.
36. DiNonno JM, Cheatwood F, M Hughes, et al. HIAD on ULA (HULA) Orbital Reentry Flight Experiment Concept. 13th International Planetary Probe Workshop. 2016.
37. Cheatwood FM. Hypersonic Inflatable Aerodynamic Decelerator (HIAD) Technology. *NASA's Space Administration Game Changing Technology Industry Day*.2016;29–30.
38. Hughes SJ, Cheatwood FM, Dillman RA, et al. Hypersonic Inflatable Aerodynamic Decelerator (HIAD) Technology Development Overview. *21st AIAA Aerodynamic Decelerator Systems Technology Conference and Seminar*. 2011;2524.
39. Jurewicz D, Brown G, Gilles B, et al. Design and Development of Inflatable Aeroshell Structure for IRVE-3. 21st AIAA Aerodynamic Decelerator Systems Technology Conference and Seminar. 2011;2522.
40. Lindell MC, Hughes SJ, Dixon M, et al. Structural Analysis and Testing of the Inflatable Re-entry Vehicle Experiment (IRVE). *47th AIAA/ASME/ASCE/AHS/ASC Structures, Structural Dynamics, and Materials Conference*. 2006;1699.